Supplementary Material (ESI) for Chemical Communications

A three-dimensional metal-organic framework with a distorted Kagome related layer showing canted antiferromagnetic behaviour

Partha Mahata,[a] Diptiman Sen[b] and Srinivasan Natarajan[a*]

[a] Framework Solids Laboratory, Solid State and Structural Chemistry Unit, Indian Institute of Science, Bangalore 560 012, India E-mail: snatarajan@sscu.iisc.ernet.in

[b] Centre for High Energy Physics, Indian Institute of Science, Bangalore 560 012, India

ELECTRONIC SUPPLEMENTARY INFORMATION

Table S1: Crystal data and structure refinement parameters for $[Mn_3\{C_6H_3(COO)_3\}_2]$

Empirical formula	$C_{18}H_6O_{12}Mn_3$
Formula weight	579.04
Crystal system	Monoclinic
Space group	$P2_1/n$ (no. 14)
a (Å)	11.314(3)
b (Å)	6.5962(16)
c (Å)	11.391(3)
α (deg)	90.0
β (deg)	111.029(4)
γ (deg)	90.0
Volume ($Å^3$)	793.5(3)
Z	2
T (K)	273(2)
ρ_{calc} (g cm^{-3})	2.424
μ (mm^{-1})	2.435
θ range (deg)	2.18 to 27.97
λ (Mo Kα) (Å)	0.71073
R indices [I>2σ(I)]	$R_1 = 0.0337$, $wR_2 = 0.0680$
R indices (all data)	$R_1 = 0.0425$, $wR_2 = 0.0714$

$R_1 = \Sigma ||F_0|-|F_c|| / \Sigma |F_0|$; $wR_2 = \{\Sigma[w(F_0^2 - F_c^2)^2] / \Sigma[w(F_0^2)^2]\}^{1/2}$. $w = 1/[\sigma^2(F_0)^2 + (aP)^2 + bP]$, $P = [max.(F_0^2,0) + 2(F_c)^2]/3$, where a = 0.0263 and b =0.9220

Table S2: Selected bond distances (Å) observed in $[Mn_3\{C_6H_3(COO)_3\}_2]$

Bond	Distances, Å	Bond	Distances, Å
Mn(1)-O(1)#1	2.097(2)	Mn(2)-O(6)#5	2.0845(19)
Mn(1)-O(2)#2	2.1376(19)	Mn(2)-O(6)#1	2.0845(19)
Mn(1)-O(5)#3	2.202(2)	Mn(2)-O(3)	2.1804(19)
Mn(1)-O(3)	2.2700(19)	Mn(2)-O(3)#6	2.1804(19)
Mn(1)-O(4)#4	2.3229(19)	Mn(2)-O(4)	2.1819(19)
Mn(1)-O(5)#4	2.3776(19)	Mn(2)-O(4)#6	2.1819(19)

Symmetry operations used to generate equivalent atoms for **I**: #1 x+1/2,-y+1/2,z-1/2 #2 -x+1/2,y-1/2,-z+1/2 #3 -x+1,-y+1,-z+1 #4 x-1/2,-y+1/2,z-1/2 #5 -x+1/2,y-1/2,-z+3/2 #6 -x+1,-y,-z+1

Table S3: Selected bond angle observed in $[Mn_3\{C_6H_3(COO)_3\}_2]$

Angle	Amplitude (º)	Angle	Amplitude
O(1)#1-Mn(1)-O(2)#2	83.42(8)	O(6)#1-Mn(2)-O(3)	87.96(8)
O(1)#1-Mn(1)-O(5)#3	91.23(8)	O(6)#5-Mn(2)-O(3)#6	87.96(8)
O(2)#2-Mn(1)-O(5)#3	130.30(8)	O(6)#1-Mn(2)-O(3)#6	92.04(8)
O(1)#1-Mn(1)-O(3)	99.18(7)	O(3)-Mn(2)-O(3)#6	180.0
O(2)#2-Mn(1)-O(3)	147.08(8)	O(6)#5-Mn(2)-O(4)	95.11(8)
O(5)#3-Mn(1)-O(3)	82.59(7)	O(6)#1-Mn(2)-O(4)	84.89(8)
O(1)#1-Mn(1)-O(4)#4	156.12(8)	O(3)-Mn(2)-O(4)	85.61(7)
O(2)#2-Mn(1)-O(4)#4	87.50(7)	O(3)#6-Mn(2)-O(4)	94.39(7)
O(5)#3-Mn(1)-O(4)#4	77.94(7)	O(6)#5-Mn(2)-O(4)#6	84.89(8)
O(3)-Mn(1)-O(4)#4	100.41(7)	O(6)#1-Mn(2)-O(4)#6	95.11(8)
O(1)#1-Mn(1)-O(5)#4	143.87(7)	O(3)-Mn(2)-O(4)#6	94.39(7)
O(2)#2-Mn(1)-O(5)#4	81.77(7)	O(3)#6-Mn(2)-O(4)#6	85.61(7)
O(5)#3-Mn(1)-O(5)#4	123.18(6)	O(4)-Mn(2)-O(4)#6	180.0
O(3)-Mn(1)-O(5)#4	77.05(7)	Mn(2)-O(3)-Mn(1)	97.88(7)
O(4)#4-Mn(1)-O(5)#4	55.19(6)	Mn(2)-O(4)-Mn(1)#9	130.53(8)
O(6)#5-Mn(2)-O(6)#1	180.0	Mn(1)#3-O(5)-Mn(1)#9	112.28(8)
O(6)#5-Mn(2)-O(3)	92.04(8)		

Symmetry operations used to generate equivalent atoms for **1**: #1 x+1/2,-+1/2,z-1/2 #2 -x+1/2,y-1/2,-z+1/2

#3 -x+1,-y+1,-z+1 #4 x-1/2,-y+1/2,z-1/2 #5 -x+1/2,y-1/2,-z+3/2 #6 -x+1,-y,-z+1 #9 x+1/2,-y+1/2,z+1/2

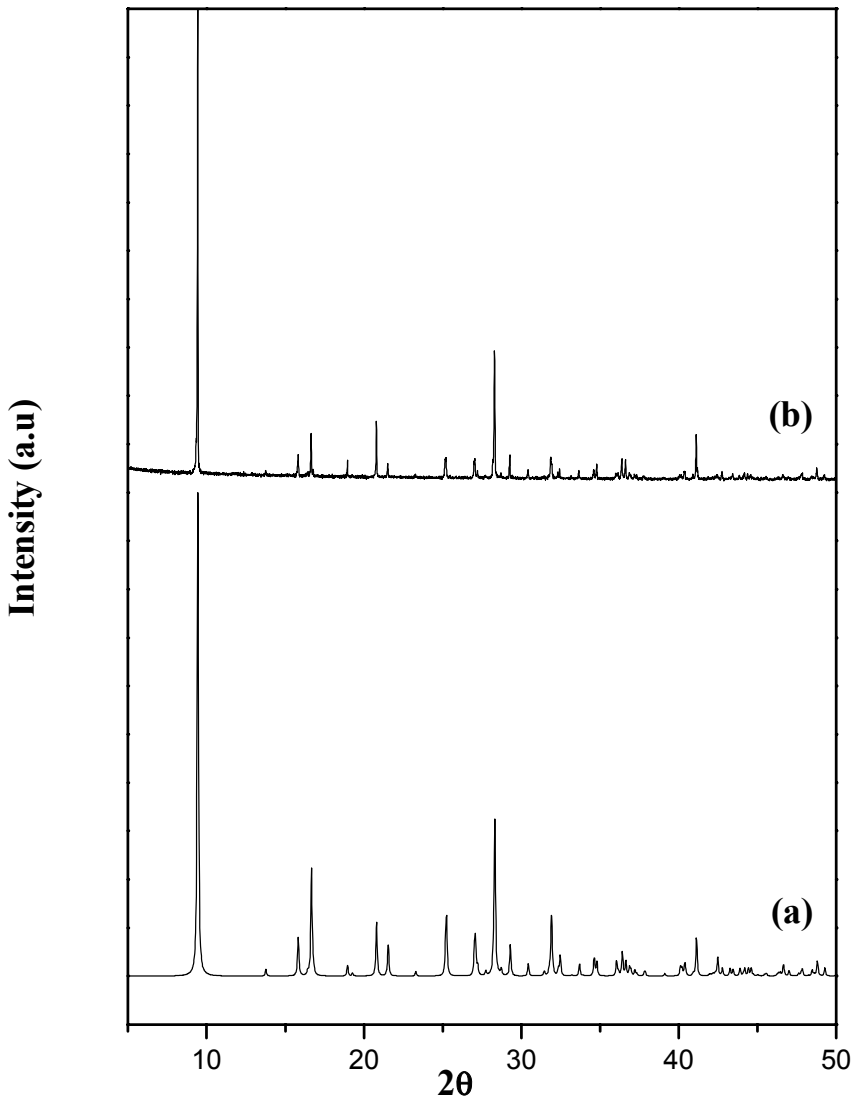

Fig. S1: Powder XRD (CuKα) pattern of $[Mn_3\{C_6H_3(COO)_3\}_2]$, (a) simulated and (b) experimental

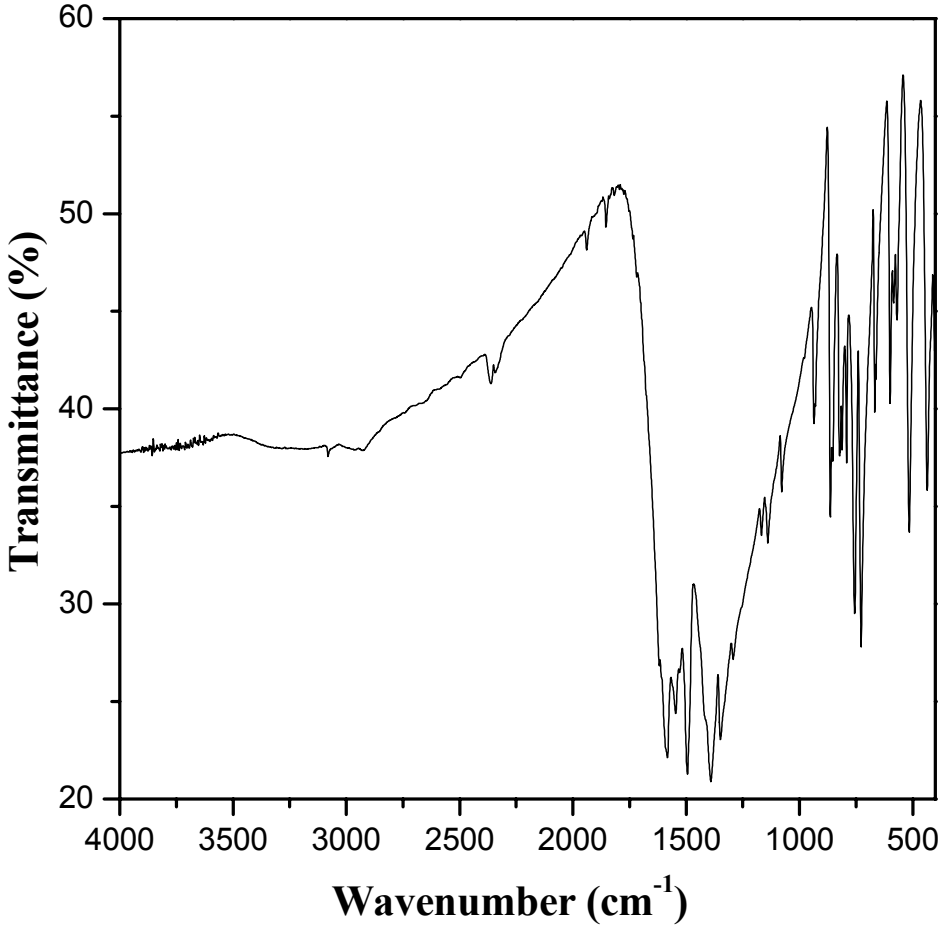

Fig. S2: IR spectra of $[Mn_3\{C_6H_3(COO)_3\}_2]$

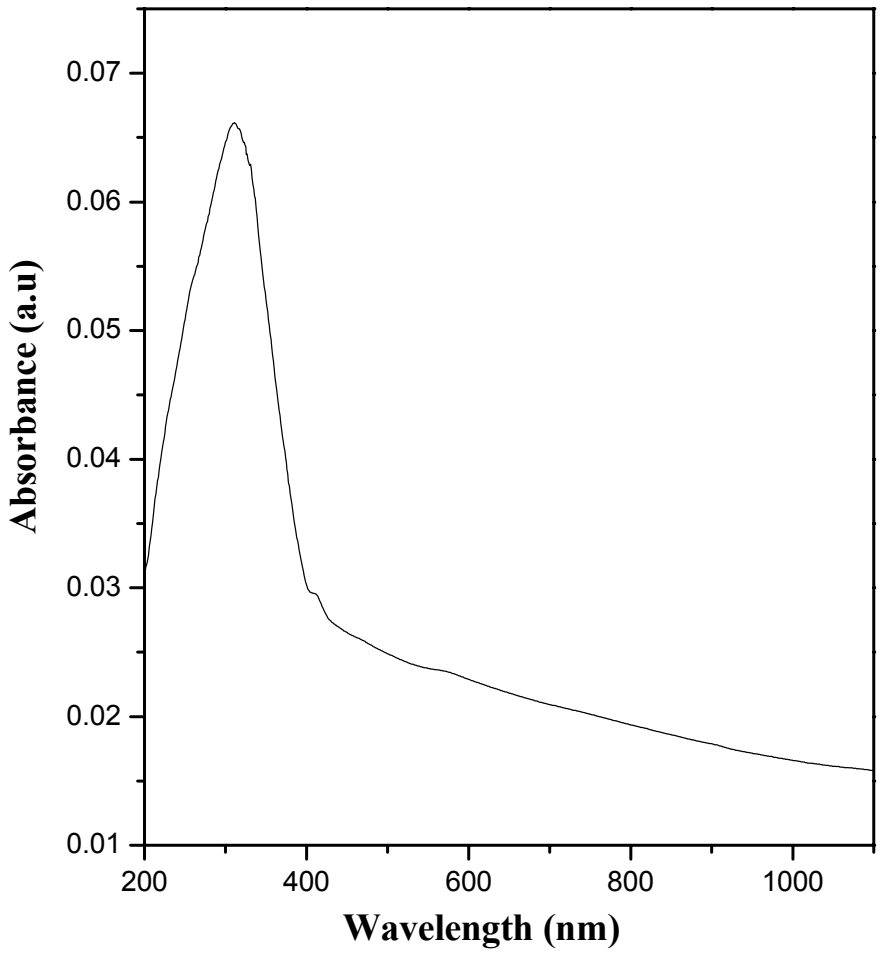

Fig. S3: UV spectra of $[Mn_3\{C_6H_3(COO)_3\}_2]$

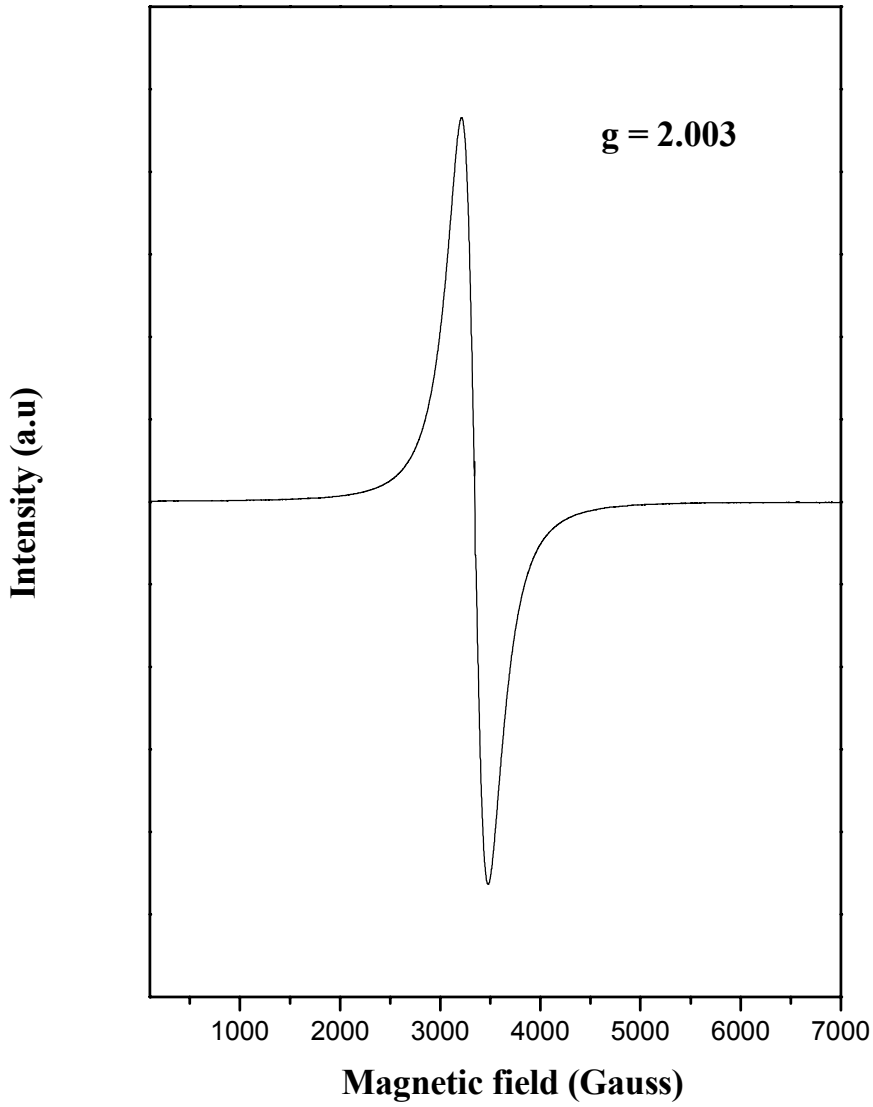

Fig. S4: EPR spectra of $[Mn_3\{C_6H_3(COO)_3\}_2]$

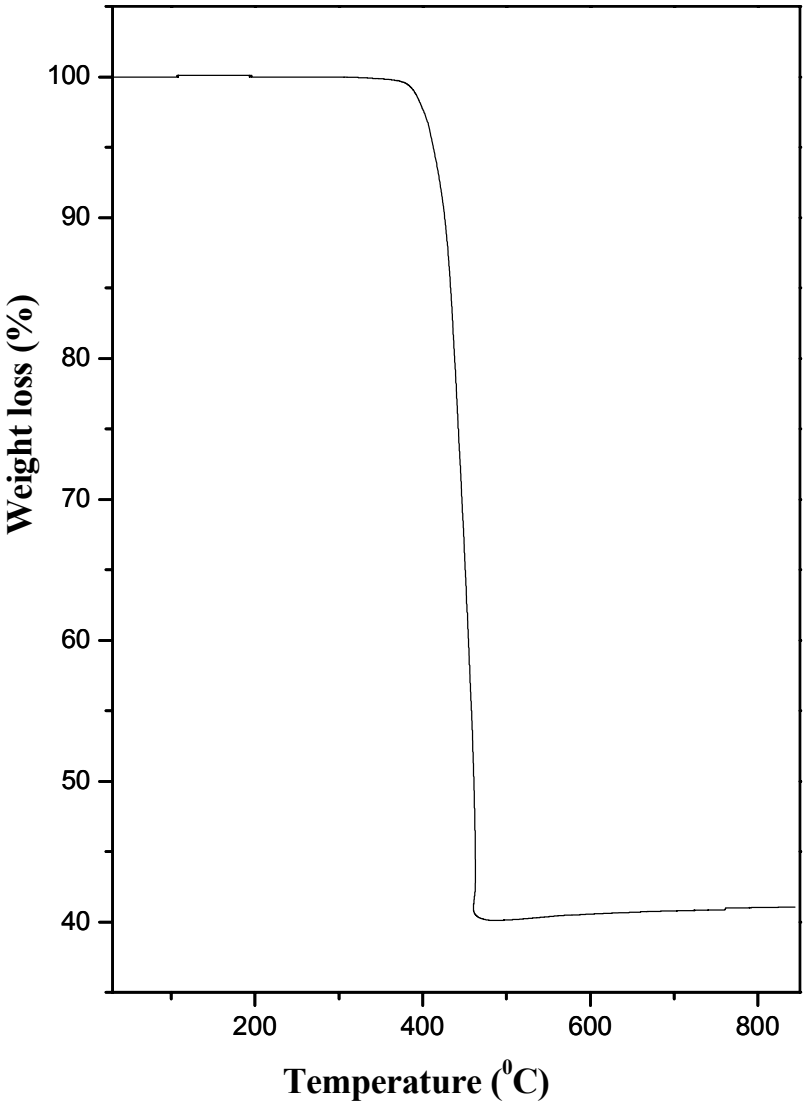

Fig. S5: TGA studies of $[Mn_3\{C_6H_3(COO)_3\}_2]$ in air

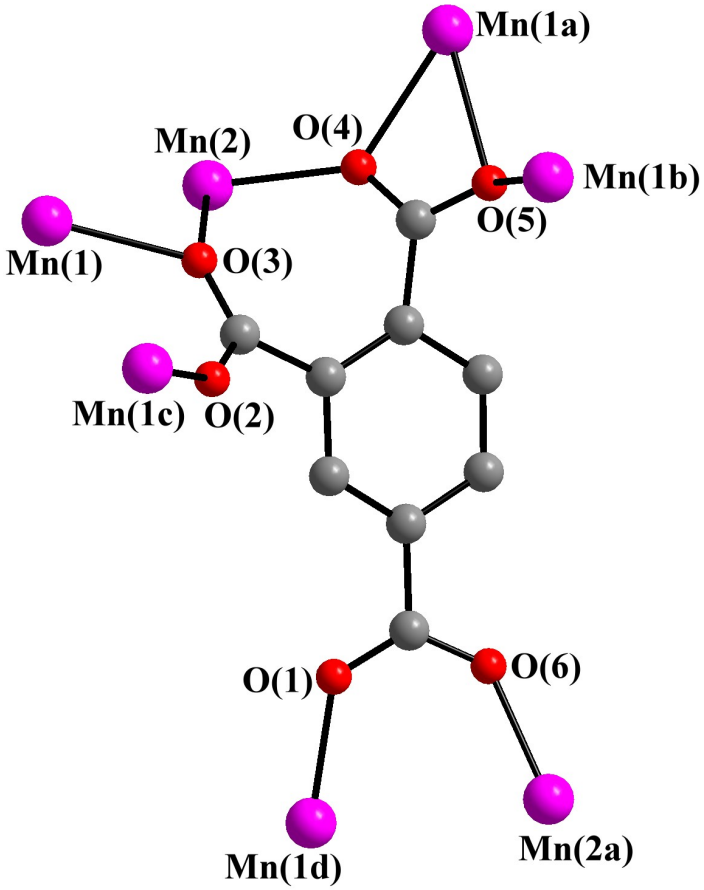

Fig. S7: Figure shows the coordination mode of trimillitate anions in $[Mn_3\{C_6H_3(COO)_3\}_2]$, Symmetry operation: Mn(1a) x+1/2, -y+1/2, z+1/2, Mn(1b) –x+1, -y+1, -z+1, Mn(1c) –x+1/2, y+1/2, -z+1/2, Mn(1d) x-1/2, -y+1/2, z+1/2, Mn(2a) –x+1/2, y+1/2, -z+3/2

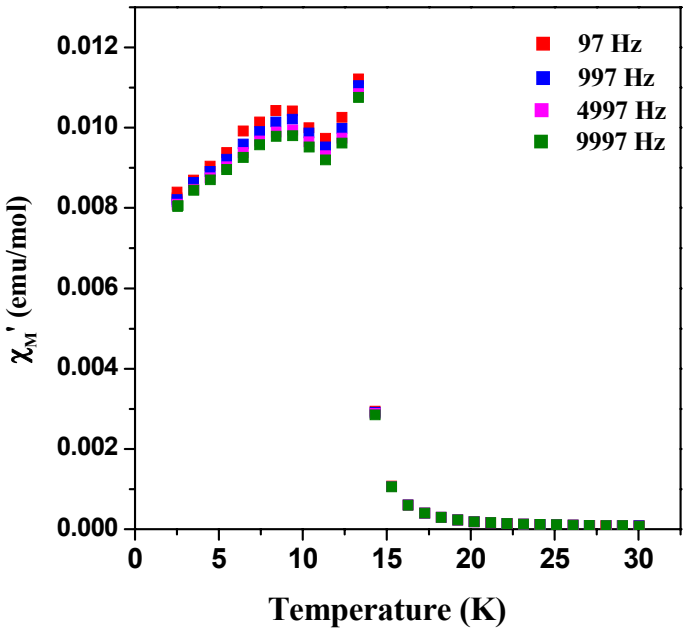

(a)

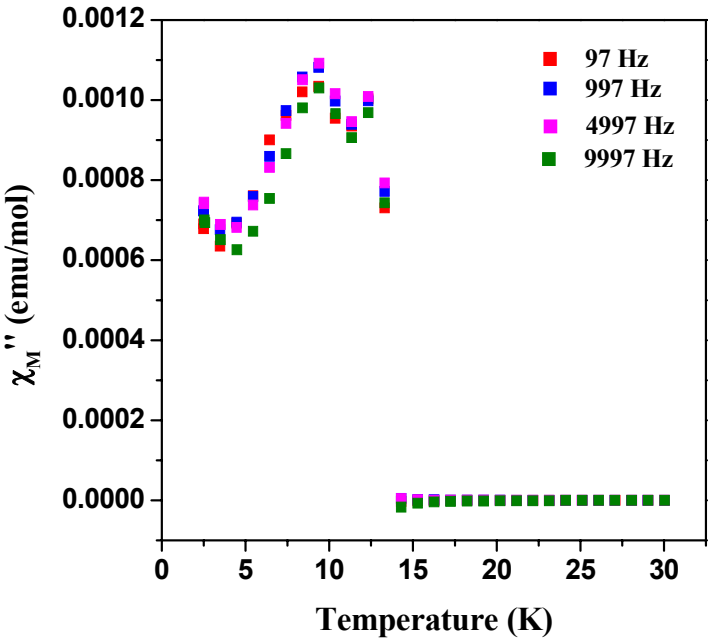

(b)

Fig. S8: Frequency dependence of the AC molar magnetic susceptibility of $[Mn_3\{C_6H_3(COO)_3\}_2]$ (a) in-phase signal, (b) out-of-phase signal. Note that the transition at around 13 K in both cases.